Electromagnetic properties of graphene nanoplatelets/epoxy composites

A. Plyushch [a, *], J. Macutkevic [a], P. Kuzhir [b, c], J. Banys [a], Dz. Bychanok [b, d], Ph. Lambin [e],
S. Bistarelli [f], A. Cataldo [f], F. Micciulla [f], S. Bellucci [f]

[a] Faculty of Physics, Vilnius University, Sauletekio 9, Vilnius LT-10222, Lithuania
[b] Research Institute for Nuclear Problems of Belarusian State University, Bobruiskaya Str. 11, Minsk 220030 Belarus
[c] Tomsk State University, 36 Lenin Prospekt, Tomsk 634050, Russian Federation
[d] Ryazan State Radio Engineering University, 59/1 Gagarina Street, Ryazan 390005, Russian Federation
[e] Physics Department, FUNDP - University of Namur, 61 rue de Bruxelles, 5000 Namur, Belgium
[f] INFN-Laboratori Nazionali di Frascati, Via E. Fermi 40, 00044 Frascati, Italy

ARTICLE INFO

Keywords:
Polymer-matrix composites (PMCs)
Nano particles
Electrical properties
Thermal properties
Annealing

ABSTRACT

Results of broadband dielectric spectroscopy of epoxy resin composites containing graphene nanoplatelets (GNP) are presented in a wide temperature range (25–500 K). The as-produced composites were heated at temperatures above the epoxy glass transition and subsequently cooled down to room temperature. This annealing was proved to be a simple but powerful process to improve significantly the electromagnetic properties of the GNP-based composites. The dc conductivity of epoxy filled with 4 wt% GNP is 68 times higher after annealing. Another benefit of the annealing is to lower substantially the percolation threshold, from 2.3 wt% for as-produced samples to 1.4 wt%. In composites above the percolation threshold, the electrical conductivity is the result of tunneling between GNP clusters. For a given GNP concentration, the tunnel barrier decreases after annealing.

1. Introduction

Polymer composite mixing bulk specific properties of the matrix—flexibility, resistance to corrosion, good processability, strong adhesion to different substrates, curing ability etc—and conducting properties from the fillers (ferrites, noble metals, carbon and graphite nano- and microstructures) have received a lot of attention during the last two decades [1]. These advanced materials find more and more applications in aerospace, automotive, energy, electronics, defense and health care sectors [2]. Among others, one of the most promising fillers used to produce conductive polymer composites is carbon in various forms: carbon black [3], graphene [4], microsized quartz coated by graphene [5] vapor-grown carbon fibers [6], multi-walled and single-walled carbon nanotubes [7,8], onion-like carbon [9]. A reason for that is the light weight, the chemical resistance and the high dc and ac conductivity of those structures.

To explore the electromagnetic (EM) applications of composites, it is important to measure and analyze their electrical conductivity and effective permittivity. Several theoretical models can be used for the analysis, such as the percolation theory [10], Maxwell—Garnett [11] and McLachlan [12] effective medium theories, and the generalized McLachlan-Jonsher theory [13]. The latter makes it possible to describe the frequency and concentration dependence of the complex effective permittivity. In parallel, computer simulations methods become more and more efficient nowadays to predict the EM properties of composites. Novel methods of calculation allow taking into account the geometry of filler [14] and it influence on AC conductivity of composite [15], make possible performing simulations for a wide range of volume fractions, permittivity ratios and packing conditions [16]. Many researchers have examined this subject by performing *ab-initio* calculations, for example with density functional theory (DFT) [17], or finite-element method (FEM) [18,19] and a combination of FEM and Monte-Carlo simulations [20,21].

Carbon nanotubes (CNT) based composites are extremely interesting for conductive applications. CNTs lead to very low percolation threshold (0.03–0.5 wt% depending on the CNT origin,

* Corresponding author.
E-mail address: artyom.plyushch@gmail.com (A. Plyushch).

the wall surface quality, the functionalization, the dispersion state) and yield huge effective permittivity and electrical conductivity values at all frequencies [22] including microwave and terahertz ranges. However, a drawback of carbon nanotubes is their higher cost in comparison with other carbon nanostructures such as different derivatives of graphite. Another serious disadvantage is the possible toxicity of CNTs, which has been debated for long [23]. This problem seems less critical with bigger and/or less slender carbon particles such as graphene nanoplatelets (GNP) [24].

GNPs are carbon nanostructures consisting of small stacks of graphene sheets with overall thickness from 1 nm to a few tens of nanometers, and lateral linear dimensions from a few micrometers up to hundreds of micrometers [25]. Graphene nanoplatelets are produced by thermal exfoliation of graphite intercalated compounds [26]. By contrast with CNTs, the GNP production process is easy and cheap. Without a proper surface treatment, GNPs might have poor interfacial adhesion with polymers because of lack of chemical bonding [24,27]. GNP functionalization can lead to better interfacial adhesion to polymer that improves mechanical [28] and thermal [29] properties of resultant composite, but at same time may deteriorate its electrical conductivity. Chemical treatments have been demonstrated improving the strength of interfacial interactions [30,31] without changing significantly the EM properties of their composites [24].

Exploring the EM properties of nanocarbon-based composites at low temperatures (below 300 K) is very important, for it gives information on the main electrical transport mechanism [7,32–34]. Also, the variation of EM properties of polymer/carbon composites with temperature are worth studying due to irreversible processes occurring near and above the glass transition temperature of the polymer matrices [35–37]. In this respect, the hysteresis of electromagnetic properties on heating and cooling cycles has already been reported for composites with carbon black [38], onion-like carbon [9] and CNTs [39]. Moreover, above the room temperature the electrical conductivity and the effective permittivity of composites above the percolation threshold can increase or decrease with temperature [40,41]. These effect can be related with particles redistribution or polymer matrix conductivity.

The objective of the present work was to check with complementary tools whether a thermal treatment may have significant and positive effects on the EM properties of epoxy resin loaded with small amounts of GNPs (up to 4 wt%). The paper is organized as follows: All the experimental details are collected in Section II. The results of broadband dielectric spectroscopy performed at room temperature (subsection A), high (subsection B) and low (subsection C) temperature are discussed in Section III. Conclusions are drawn in Section IV.

2. Experimental

Graphene nanoplatelets were produced by micro-cleavage exfoliation of expanded graphite. Expandable graphite was provided by Asbury® https://asbury.com/. Expandable graphite is manufactured by treating the flake graphite with various intercalation reagents that migrate between the graphene layers in a graphite crystal and remain as stable species. When exposed to a rapid increase of temperature, these intercalation compounds decompose into gaseous products as the result of high interlayer pressure. The internal stress is strong enough to push apart graphite basal planes along the *c* axis. Asbury expandable graphite exhibits a micro and submicron lamellar structure, an example of which revealed by SEM is shown in Fig. 1 (a). After micro-cleavage exfoliation, induced by microwave irradiation [42–46], a porous structure is visible in the SEM micrograph reproduced in Fig. 1 (b). A gentle treatment with ultrasound bath destroys the superstructure, releasing GNP.

In this work, series of composite samples were produced using Epikote 828, a curing agent called A1 (i.e., a modified TEPA) and 0.25, 1, 2, 3 and 4 wt% of GNP filler. The procedure of composite manufacturing is described in details elsewhere [8,38]. In summary, the resin was degassed under vacuum (1–3 mbar) for 12–14 h, then was put into an oven at 65° C. In the meantime, the GNPs were dispersed in propanol, and the suspension was submitted to an ultrasonic bath for 1.5 h. Afterwards, the alcoholic suspension of GNPs was mixed with the resin. The obtained mixture was placed inside an oven at 130–150° C for evaporating the alcohol. The curing agent A1 was added to the mixture of resin and filler through slow manual mixing for about 7 min. The blend was then poured into molds of dimensions $1 \times 1 \times 7$ cm^3, and left as such for 20 h for the curing process at room temperature, and finally 4 h in an oven at 80° C. When the process was completed, the samples were removed from the molds. After curing at room temperature, the samples were treated for 4 h in an oven at 353 K.

Dielectric properties of the samples where measured in the frequency range 20 Hz–1 MHz with a LCR HP4284A meter. For low-temperature measurements (25–300 K), the samples were placed in the closed-cycle cryostat. Measurements at high-temperature (300–500 K) were performed in a home-made furnace. All measurements were performed in air with heating/cooling rate 1 K/min without isothermal annealing. The samples cut from the $1 \times 1 \times 7\ cm^3$ molded composite had a thickness of about 2 mm and the square-shaped cross section of area 30 mm^2. Silver paste was applied for contacting.

In the frequency range 1 MHz–3 GHz, two different experimental setups were used depending on the GNP concentration. Samples containing 2 wt% and more GNP were analyzed by a coaxial dielectric spectrometer with vector network analyzer Agilent 8714ET. Here, sample with typical area of 2 mm^2 and thickness of 0.3 mm were studied. Epoxy composites with lower GNP concentration were analyzed with E5071C ENA Network Analyzer setup. For measurements of the scattering *S* parameters, an airline cell containing toroidal sample was placed in coaxial line between two ports of the vector network analyzer. The standard procedure was used to convert the *S* parameters into the complex permittivity ε of the material [47].

The microwave measurements in the 26–37 GHz frequency range (K_a-band) were carried out with a scalar network analyzer R2-408R (ELMIKA, Vilnius, Lithuania). For small concentrations (2 wt% and lower), parallelepiped samples of typical thicknesses 1.2 mm were precisely cut to fit the waveguide cross section. Samples with higher concentrations were shaped in cylinders of diameter $d = 0.4$ mm. The EM response of the composites were measured as the ratios of transmitted/input (S_{21}) and reflected/input (S_{11}) signals. The conductivity was recalculated from the *S* parameters via methods described elsewhere [48,49]. For shielding measurements 2 mm thick parallelepiped samples were precisely cut to fit the waveguide cross section 7.2 mm × 3.4 mm. The reflectance(R), the transmittance (T) and the absorbance (A) were calculated from S-parameters in following way: $T = S_{21}^2$, $R = S_{11}^2$, $A = 1 - R - T$.

Measurements at frequencies ranging from 100 GHz to 2 THz were performed in transmission mode using a time-domain THz spectrometer TERAVIL T-SPEC based on an femtosecond laser system. Large-area, polished parallel plates of 0.5 mm-thickness were investigated.

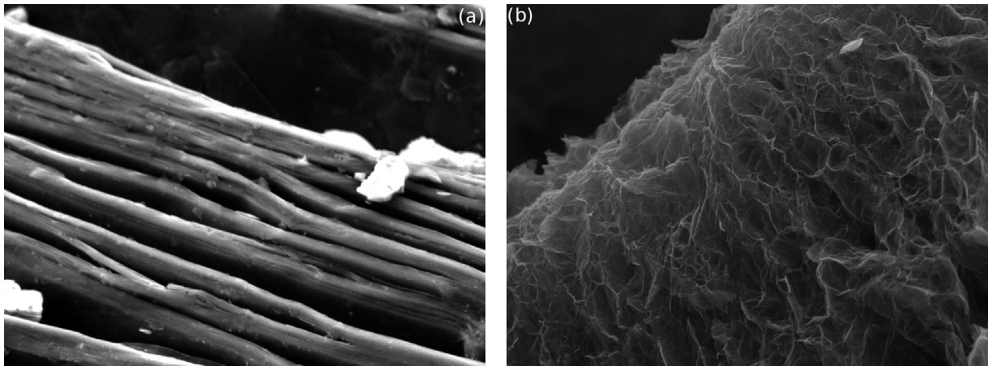

Fig. 1. Lamellar structure of expandable graphite (a) and (b)worm-like GNP structure after exfoliation process.

3. Result and discussion

3.1. Room temperature

The frequency dependence of the real part of the effective permittivity and the conductivity measured at room temperature is presented in Fig. 2.

Both the static effective permittivity and dc conductivity increase with increasing concentration of GNPs and reach 300 and 3 mS/m respectively for composite with 4 wt% of GNP inclusions. For these composites the low frequency dispersion of the real and the imaginary part of the permittivity can be described by Jonsher law [50,51]:

$$\begin{cases} \varepsilon^* \sim (-i\omega\tau)^{n_1-1}, & \omega > \omega_c, \\ \varepsilon^* \sim (-i\omega\tau)^{n_{lfd}-1}, & \omega < \omega_c, \end{cases} \tag{1}$$

where $\omega=2\pi\nu$ is the angular frequency ω_c is the critical frequency, $n_{lfd}<n_1<1$. Below 10 kHz a frequency independent conductivity (dc-conductivity) is observed for epoxy loaded with 3 and 4 wt% GNP. In this case the conductivity can be described as a sum of dc- and ac-conductivity terms. Since $\sigma = \varepsilon''\varepsilon_0\omega$, the imaginary part in Eq. (1) can be presented as (Fig. 2 (b), solid curves) [52]:

$$\sigma = \sigma_{dc} + \sigma_{ac}(\omega), \tag{2}$$

where σ_{dc} is the dc conductivity and $\sigma_{ac}(\omega)$ is the ac conductivity.

The data indicate that the critical concentration between two conduction regimes lies between 2 and 3 wt% GNPs. Its value can be evaluated using the usual formula describing the conductivity σ *versus* the filler concentration p_{GNP} near the percolation threshold p_c [53]:

$$\begin{cases} \sigma = \sigma_0 \left(\dfrac{p_{GNP} - p_c}{p_c} \right)^{-s}, & p < p_c, \\ \sigma = \sigma_i \left(\dfrac{p_c - p_{GNP}}{p_c} \right)^{t}, & p_{GNP} > p_c, \end{cases} \tag{3}$$

where σ_0 is the matrix conductivity, σ_i is the inclusions conductivity, s and t is the critical exponents.

Fitting the conductivity of the epoxy composites below the percolation threshold i.e. 0, 0.25, 1 and 2 wt% with first equation of Eq. (3) at a fixed frequency, here 117 Hz, yields $p_c = 2.3$ wt% and $s = 1.8$. The critical exponent exhibits slightly higher value than universal one [53,54]. Such values can be also found in variety of composite materials [55,56] and can be explained by inverse Swiss cheese model [54].

3.2. High temperature

The epoxy resin becomes conductive at high temperature. As a result, a dc plateau was observed in the conductivity frequency spectra of all composites, above and below the percolation

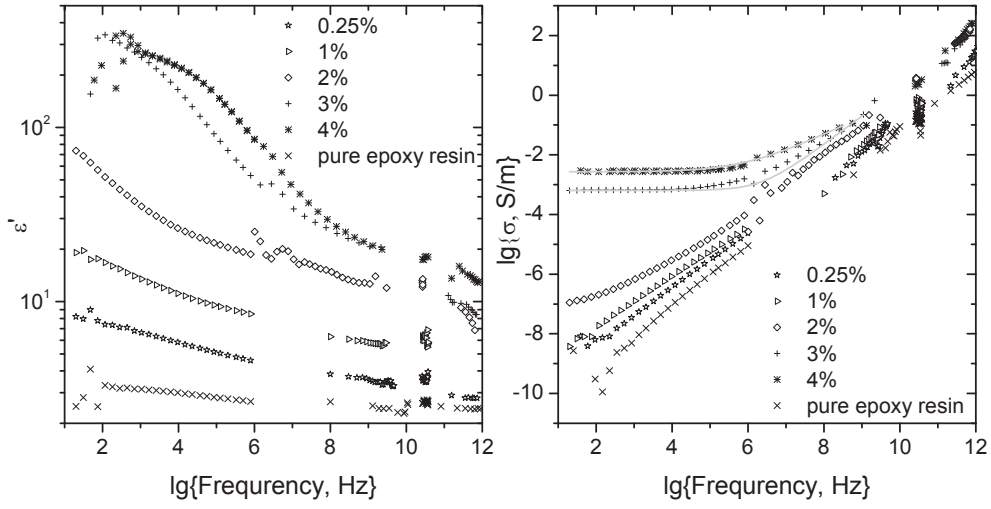

Fig. 2. Real part of the effective permittivity (left) and conductivity (right) of epoxy resin and GNP/epoxy composites against frequency for different concentrations in log–log scale.

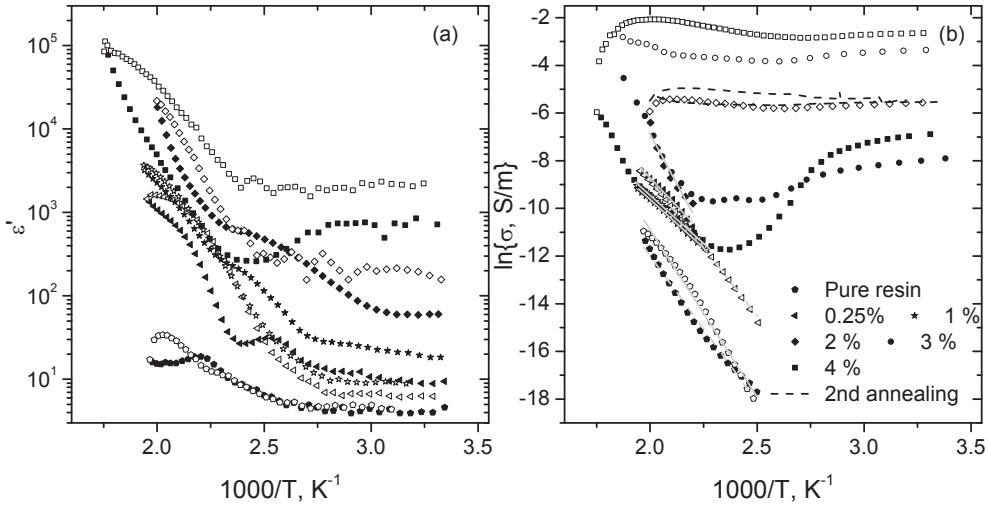

Fig. 3. Temperature dependence of (a) the effective permittivity at 129 Hz and (b) the dc electrical conductivity measured on heating (solid symbols) and on cooling (open symbols) composite samples with different GNP concentrations.

threshold. The temperature variation of the permittivity and the dc conductivity of samples is presented on Fig. 3 (b).

The dc conductivity of composites with a low concentration of GNP (0.25 and 1 wt%) demonstrates some small hysteresis on heating and cooling, and can be fitted with Arrhenius law. For composites above the percolation threshold (3 and 4 wt%), three different dc conductivity regimes can be identified on heating: 1) at low temperatures (below 360 K), the dc conductivity is almost temperature independent; 2) in the intermediate temperature region—about 360 K–390 K for the composite with 4 wt% GNP—the dc conductivity decreases with increasing temperature due to thermal expansion of the epoxy matrix, which slightly increases the distance between conductive clusters; 3) at higher temperatures (above the glass transition in pure epoxy resin), the dc conductivity of the composites increases due to the finite conductivity of the epoxy matrix. A huge hysteresis between the first cooling and the first heating cycle is observed for composites filled with 2, 3 and 4 wt % of GNP. The hysteresis is followed by a drastic increase of the composite conductivity (up to six orders of magnitude). In addition, after annealing, the variation of the dc conductivity with T becomes more flat. Moreover, the sample with 2 wt% GNP has acquired a dc conductivity plateau at room temperature after annealing. The percolation concentration recalculated with second Eq. (3) for percolated samples (2,3,4 *wt.* %) gives $p_c = 1.4$ wt %. In other words, the percolation threshold has decreased substantially after annealing the samples. It is worth mentioning that the dc conductivity only slightly increases after a subsequent heating-cooling treatment (dashed-line curves in Fig. 3) and saturates after a few cycles.

It was observed that GNP/epoxy composites lead to substantial EM attenuation in the microwave domain and are therefore interesting materials for shielding applications. A 2-mm thick sample with 4 wt% transmits only 14% of initial radiation. Table 1 shows that annealing the samples improves their shielding ability significantly: the transmittance of the sample with 2 wt% shifts form 22%–15% and from 14% to 8% for the 4 wt% sample. However, variation of shielding behaviour is not the same for both compositions: for 2 wt%, sample annealing increases the reflection and slightly decreases the absorption whereas for 4 wt%, the reflection remains unchanged and the absorption increases.

Table 1
Shielding efficiency of 2 mm-thick composite layer at 30 GHz frequency.

Sample	Reflectance, %	Transmittance, %	Absorbance, %
2%	45	22	33
2%, annealed	57	15	28
4%	70	14	16
4%, annealed	71	8	21

The sample impedance (i.e. the reciprocal of the complex conductivity):

$$\rho^* = \frac{1}{i\omega\varepsilon_0\varepsilon^*} = \frac{1}{i\omega\varepsilon_0(\varepsilon' - i\varepsilon'')}, \tag{4}$$

extracted from the permittivity data was employed to understand the observations. The frequency dependence of the measured impedance displayed in Fig. 4 cannot be described by that a single RC circuit $\rho^*=R/(1+i\omega RC)=R/(1+i\omega\tau)$ (which form is very similar to the Debye equation for the dielectric dispersion). Instead, the Maxwell–Wagner relaxation of the impedance spectra was modeled by considering an infinite chain of RC circuits connected in series. The distribution $f(\tau)$ of relaxation times was calculated by solving the integral equation (Eq. (5)) with the Tikhonov regularization technique [57]:

$$\rho^* = \rho_\infty + \Delta\rho \int_{-\infty}^{\infty} \frac{f(\tau)}{1 + i\omega\tau} \mathrm{d}(\ln\tau). \tag{5}$$

As we can see from Fig. 4, Eq. (5) well fits impedance spectra at higher frequencies and lower temperatures (for example above 1 kHz at T = 425 K). At higher temperatures and lower frequencies an additional dispersion is observed, which is caused obviously by non ohmic contacts.

The results are displayed in Fig. 5 for a composite sample containing 2 wt% GNP. The maximum of $f(\tau)$ shifts to shorter relaxation times upon heating the samples and the distribution becomes narrower. Upon cooling (Fig. 5 (b)), the distribution of relaxation times stays almost temperature independent and peaks at $2.5\cdot10^{-6}$ s. The results for samples with 3 and 4 wt% GNP (not shown) have a similar behaviour as for 2 wt %, but the maximum of the imaginary part of their impedance shifted at higher frequencies. For all the compositions studied, the distributions of relaxation time are almost temperature-independent after the second and

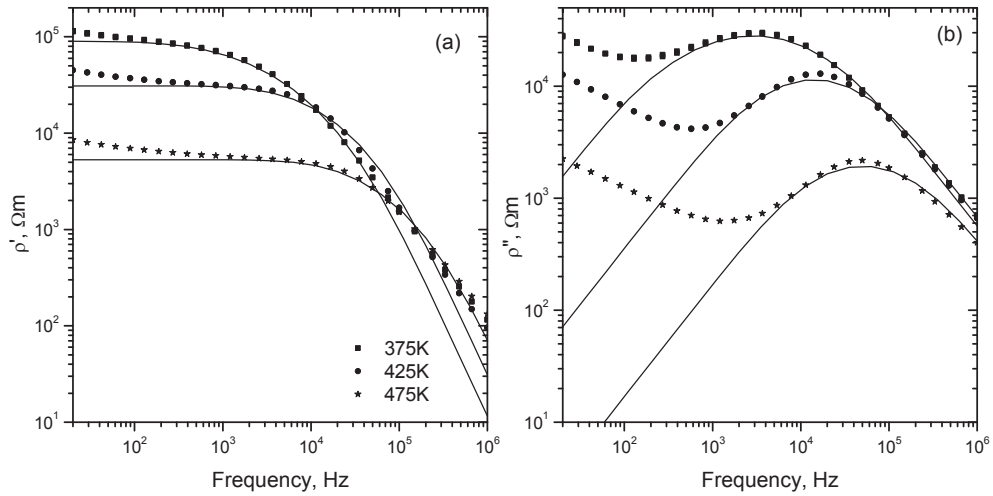

Fig. 4. Real and imaginary parts of the impedance of a GNP/epoxy sample containing 2 wt% filler for three temperatures: experimental data (symbols) and calculated with Eq. (5) (curves).

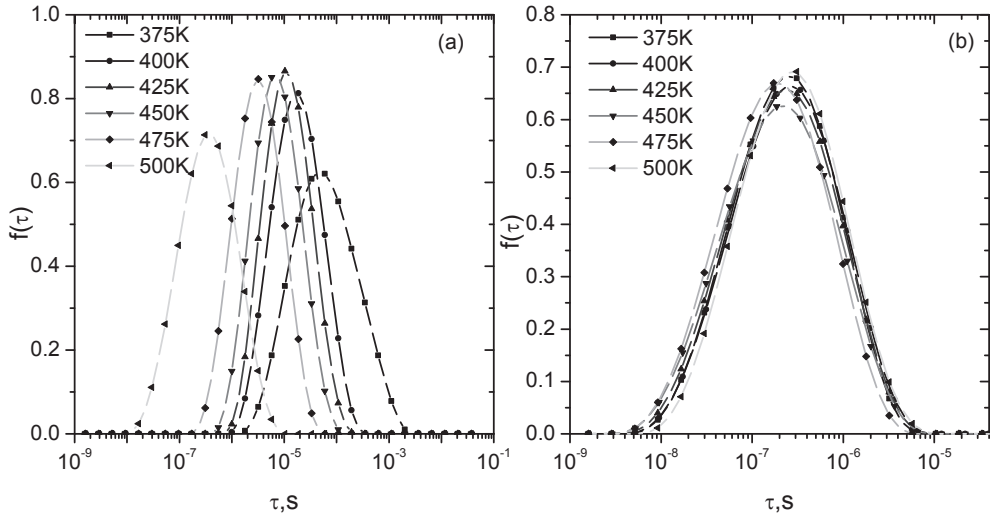

Fig. 5. Distribution of relaxation times against logτ upon heating (a) and upon cooling (b) of composites with 2 wt% GNP.

third annealing.

The relaxation time $\tau = RC \sim C/\sigma$ involves the capacitance C of a GNP cluster and the tunneling conductivity σ between neighborhood GNP clusters. The capacitance dependents only on the geometry of the GNP clusters. Assuming a spherical shape, which for GNP is a rough approximation aimed at capturing the underlying physics, $C = 4\pi\varepsilon_0 r$ where r is an effective radius. The tunneling conductivity between GNP clusters is dependent on their distribution inside the polymer matrix and on the GNP shape distribution. Schematically, short relaxation times come from small GNP clusters and short distances that charge carriers have to tunnel through. Long relaxation times is dominated by large GNP clusters and long distance between them. From the distribution of relaxation of times shown in Fig. 5, it is difficult to extract the exact GNP cluster shape distribution. One can nevertheless deduce that, during heating, large GNP clusters separate into smaller ones and their distribution becomes more homogeneous (see Fig. 6). A better dispersion of small clusters decreases the tunnel barrier because the distribution of the distance between them becomes narrower. Decreasing the probability of long path across the epoxy matrix increases the tunnel conductivity in annealed samples. Moreover, the conductivity activation energy deduced by Arrhenius fit decreases with increasing GNP concentration, except at the concentration 2 wt% (Table 2).

What is an impact of composite annealing on the electromagnetic properties at different frequencies? It is possible to separate two cases: 1) The low frequency approximation, $\omega\tau_{max} \ll 1$ (where τ_{max} is the most probable relaxation time). In this case according to Eq. (5), $\rho' = \rho_\infty + \Delta\rho$ and ρ'' is very small. Under such conditions and according to Eq. (4) $\varepsilon'' \gg \varepsilon'$ and $\varepsilon'' = \frac{\sigma_{dc}}{\omega\varepsilon_0}$. 2) The high frequency approximation, $\omega\ \tau_{max} \gg 1$. According to Eq. (5), $\rho' = \rho_\infty$ and ρ'' is again very small. In this case $\varepsilon' = \varepsilon_\infty$ (where ε_∞ is caused by phonons and the electronic polarization) and $\varepsilon'' = 1/(\rho_\infty \omega \varepsilon_0)$ are both very small and almost temperature independent. The highest impact of annealing is observed in low frequency region 1) due the increase in dc conductivity, while in high frequency region 2) the impact is negligible small. In intermediate frequency range, when $\omega\tau_{max} \approx 1$, the impact of the annealing is also observed (Table 1), however lower than for dc regime.

The hypothesis that breaking the clusters into smaller ones by annealing could increase the conductivity of the composite samples can be substantiated with the results of the following model

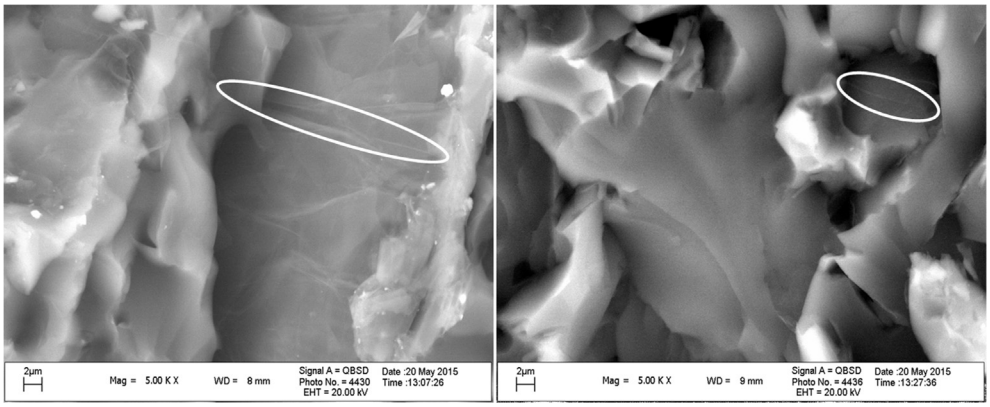

Fig. 6. SEM image of epoxy/GNP composites containing 2 wt% of GNP before (see large GNP clusters marked with white oval) and after annealing (see small GNP cluster).

Table 2
Parameters of Arrhenius law fit.

Sample,Process	$ln\sigma_0$,S/m	E_a/k_B,K	T.Region
0%, Heating [38]	12.51	12253	$T \geq 400$
0%, Cooling [38]	17.1	14000	$T \geq 400$
0.25%, Heating	10.1	9411.8	$T \geq 456$
0.25%, Cooling	13.9	11379	$T \geq 450$
1%, Heating	6.6	8112.9	$T \geq 446$
1%, Cooling	6.7	8073.9	$T \geq 440$
2%, Heating	26.5	16678	$T \geq 454$
3%, Heating	26,1	1638	$T \geq 445$
4%, Heating	11,49	1032,74	$T \geq 440$

computation. Spherical clusters, with uniform radius, were randomly distributed in a cubic cell with periodic boundary conditions. The volume filling fraction was chosen at $\eta = 0.27$, which corresponds to 2 wt% concentration of GNPs in epoxy resin at room temperature. The distribution $g(\delta)$ of closest approach distances δ between spheres was computed and averaged over many independent configurations. The precise definition of this distribution function can be found in Eq. (2) of ref. [58]. The calculations were performed for two radii R differing by a factor of 23, 12.6 and 10 m, as if each cluster were broken into two halves upon annealing. Fig. 7 clearly shows that the distribution $g(\delta)$ becomes narrower upon reducing radius and its maximum shifts towards smaller separation distances δ. It is not a surprise, since the theoretical function $g(\delta)$ for an equilibrium distribution of monodisperse hard spheres at a given filling fraction is a universal function of the ratio δ/R [58]. As a result, the width of the tunnel barrier between two clusters decreases with decreasing cluster size. The conductivity should therefore increase.

3.3. Low temperature region

Composites above the percolation threshold were studied at low temperatures. The temperature dependence of their dc conductivity temperature is plotted in Fig. 8. The dc conductivity of non-annealed samples with 3 and 4 wt% GNP has a maximum at 115 K. The increase of conductivity on cooling from 300 K to 115 K can be explained by the thermal contraction of the epoxy matrix, which reduces the distance between clusters. After annealing, the maximum of conductivity shifts to 170 K and the temperature curve of σ becomes more flat at higher temperature than for as-produced composites. As indicated by solid-line curves in Fig. 8, the observed conductivity behaviour below 170 K is well described by the tunneling law [59].

$$\sigma_{dc} = \sigma_0 \exp\left(-\frac{T_1}{T + T_0}\right), \tag{6}$$

where $k_B T_1$ represents the energy required for an electron to cross the insulating gap between GNP clusters and T_0 is the temperature above which thermally activated conduction over the barriers begins to occur. The parameters of the fits are listed in Table 3. Both T_0 and T_1 decrease with increasing concentration. Thus the electrical conductivity of GNP/epoxy composites is caused by the electron tunneling through the insulating epoxy matrix. The potential barrier for such a process can be calculated by Ref. [59]:

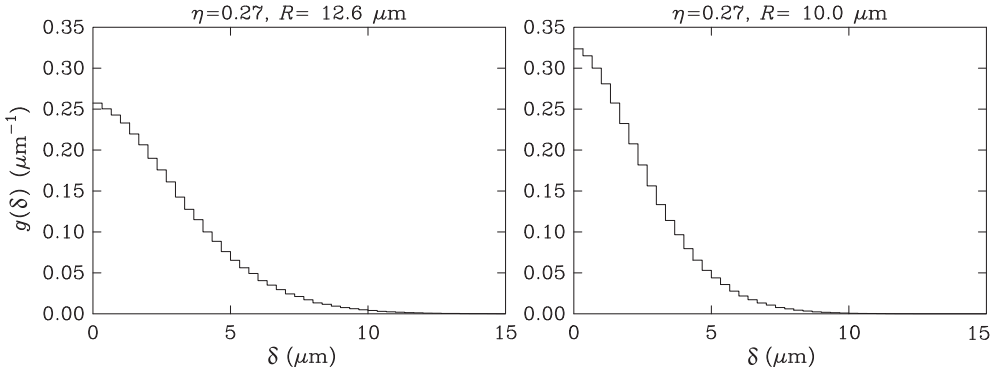

Fig. 7. Distribution of separation distances between spherical clusters of 12.6 μm and 10 μm randomly and evenly distributed in epoxy. The results of this model calculation with volume filling fraction $\eta = 0.27$ mimic the composite with 2 wt% GNP before and after annealing, respectively (see text).

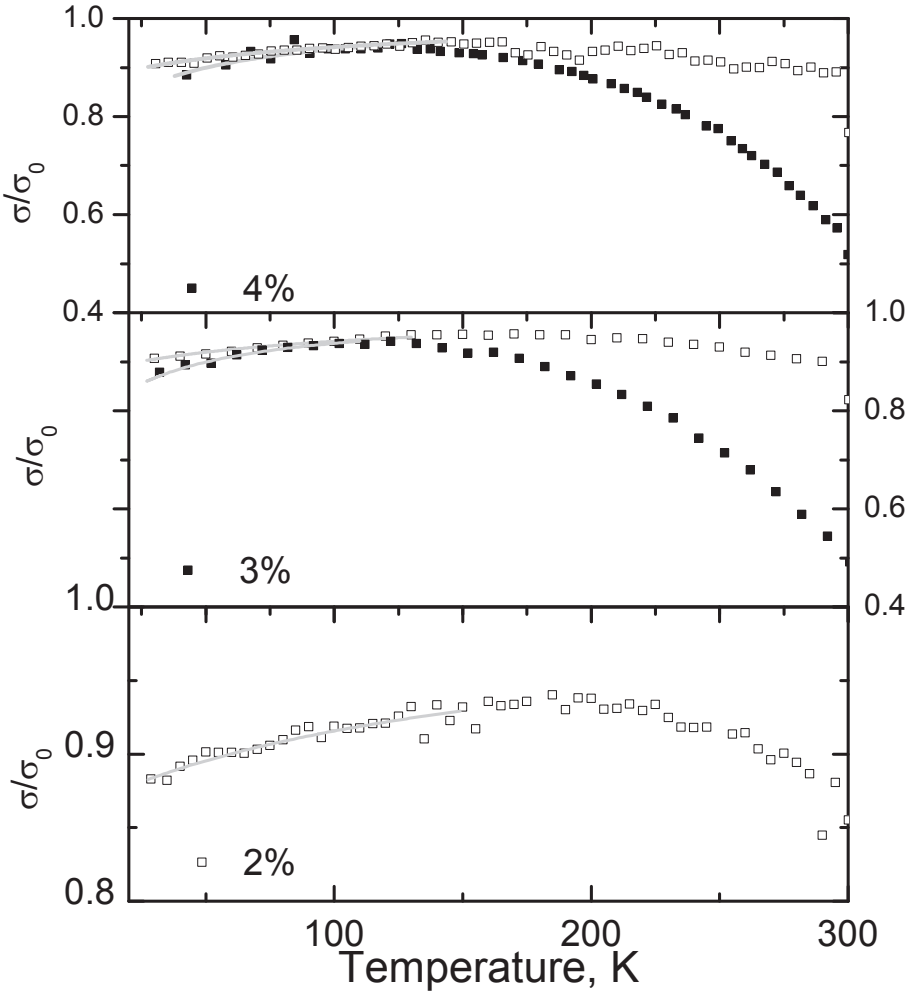

Fig. 8. Temperature dependence of dc conductivity at low temperatures of GNP/epoxy composites with 2, 3 and 4 wt% GNP. Thee open symbols represent data for annealed samples, the black symbols correspond to as-produced composites. Non-annealed composite with 2 wt% is not represented because it is below the percolation threshold.

Table 3
Parameters of tunneling law fit.

p, %	$\sigma_0 \cdot 10^3$, S/m	T_1, K	T_0, K	T_1/T_0
3%	1.26	8.25	27.79	0.30
4%	5.25	8.06	22.64	0.36
2% annealed	10.76	22.02	148.04	0.14
3% annealed	37.34	11.49	81.75	0.14
4% annealed	94.29	10.30	71.59	0.14

$$k_B T_1 = U\varepsilon_0^2, \tag{7}$$

and

$$k_B T_0 = \frac{2U\varepsilon_0^2}{\pi\chi\delta} = \frac{2k_B T_1}{\pi\chi\delta}. \tag{8}$$

In these expressions, $U{=}\delta A/8\pi$ is a measure of the tunnel junction volume, $\varepsilon_0 = 4V_0/e\delta$ is a pre-exponential factor and $\chi{=}2m_e V_0/\hbar$ is the tunneling constant for electrons, where V_0 is the potential barrier, A and ω are the junction area and thickness of the insulating gap between conductive clusters. According to Eqs. (7) and (8), $T_1/T_0 = \pi\chi\delta/2 = (\pi/2)\sqrt{2m_e/\hbar}\, V_0^{1/2}\delta$. It can be concluded from this relation that the observed decrease of the ratio T_1/T_0 by more than a factor of two after annealing (last column of Table 3) is equivalent to decreasing the potential barrier V_0 and the separation distance δ between conductive clusters. This can be understood in terms of the separation of large clusters into smaller ones and shorter average interdistance.

4. Conclusion

Electromagnetic properties of epoxy composites containing the small addition of graphene nanoplatelets have been studied over eight decades of frequency, from 20 *Hz* to 2 THz. It was demonstrated that the percolation threshold in such systems is 2.87 wt%. According to low temperature analysis, the electrical conductivity occurs by a tunneling mechanism.

During the first annealing of samples close to and above the percolation threshold, a dramatic increase of both permittivity and conductivity was observed (by a factor of 3 and by 6 orders of magnitude, respectively, in case of 2 wt% GNP). Annealing was also demonstrated to be a simple way to improve significantly the shielding ability of GNP-based composites. Indeed, as-produced composite with 4 wt% GNP provided 86% of EM attenuation across a 2 mm-thick sample, while the same sample reached 92% after annealing. The same EMI shielding efficiency of 85% can be achieved with 2 *wt.* % GNP after annealing. This phenomenon was

studied with the impedance formalism. It was found that the Maxwell–Wagner relaxation occurs. Upon heating, the relaxation time RC decreases by 3 orders of magnitude and remains unchanged on cooling. The analysis points to a redistribution of GNP clusters during which the average size and, consequently, the separation between the conductive clusters decreases. This leads to a huge rise of the conductivity and pulls the percolation threshold down to 1.4 wt%. After a second or third annealing, no significant changes of the relaxation time and the conductivity was observed, indicating that the GNP redistribution processes is achieved after the first thermal cycle.

Acknowledgments

This work is supported by the EU FP7 IRSES project FP7-318617 FAEMCAR and has benefited from EU FP7 fundings under grant NO 604391 Graphene Flagship, Federal Focus program of Ministry of Education and Science of Russian Federation # 14.577.21.0006 (project ID RFMEFI57714X0006) and Tomsk State University Competitiveness Improvement Program.

References

[1] F. Qin, C. Brosseau, A review and analysis of microwave absorption in polymer composites filled with carbonaceous particles, J. Appl. Phys. 111 (6) (2012), http://dx.doi.org/10.1063/1.3688435. http://scitation.aip.org/content/aip/journal/jap/111/6/10.1063/1.3688435.

[2] J. Liang, Y. Wang, Y. Huang, Y. Ma, Z. Liu, J. Cai, C. Zhang, H. Gao, Y. Chen, Electromagnetic interference shielding of graphene/epoxy composites, Carbon 47 (3) (2009) 922–925. http://www.sciencedirect.com/science/article/pii/S0008622308007148.

[3] B.J.-P. Adohi, A. Mdarhri, C. Prunier, B. Haidar, C. Brosseau, A comparison between physical properties of carbon black-polymer and carbon nanotubes-polymer composites, J. Appl. Phys. 108 (7) (2010), http://dx.doi.org/10.1063/1.3486491. http://scitation.aip.org/content/aip/journal/jap/108/7/10.1063/1.3486491.

[4] B.J.P. Adohi, V. Laur, B. Haidar, C. Brosseau, Measurement of the microwave effective permittivity in tensile-strained polyvinylidene difluoride trifluoroethylene filled with graphene, Appl. Phys. Lett. 104 (8) (2014), http://dx.doi.org/10.1063/1.4866419. http://scitation.aip.org/content/aip/journal/apl/104/8/10.1063/1.4866419.

[5] B.J.P. Adohi, D. Bychanok, B. Haidar, C. Brosseau, Microwave and mechanical properties of quartz/graphene-based polymer nanocomposites, Appl. Phys. Lett. 102 (7) (2013), http://dx.doi.org/10.1063/1.4793411. http://scitation.aip.org/content/aip/journal/apl/102/7/10.1063/1.4793411.

[6] I.C. Finegan, G.G. Tibbetts, Electrical conductivity of vapor-grown carbon fiber/thermoplastic composites, J. Mater. Res. 16 (2001) 1668–1674, http://dx.doi.org/10.1557/JMR.2001.0231. http://journals.cambridge.org/article_S0884291400069478.

[7] A. Mdarhri, F. Carmona, C. Brosseau, P. Delhaes, Direct current electrical and microwave properties of polymer-multiwalled carbon nanotubes composites, J. Appl. Phys. 103 (5) (2008), http://dx.doi.org/10.1063/1.2841461. http://scitation.aip.org/content/aip/journal/jap/103/5/10.1063/1.2841461.

[8] P. Kuzhir, A. Paddubskaya, D. Bychanok, A. Nemilentsau, M. Shuba, A. Plusch, S. Maksimenko, S. Bellucci, L. Coderoni, F. Micciulla, I. Sacco, G. Rinaldi, J. Macutkevic, D. Seliuta, G. Valusis, J. Banys, Microwave probing of nanocarbon based epoxy resin composite films: toward electromagnetic shielding, Thin Solid Films 519 (12) (2011) 4114–4118. http://www.sciencedirect.com/science/article/pii/S0040609011002574.

[9] J. Macutkevič, J. Banys, K. Glemža, V. Kuznetsov, V. Borjanovic, O. Shenderova, Dielectric properties of annealed onion-like carbon composites in microwave region, Lithuanian J. Phys. 53(4).

[10] A.L. Efros, B.I. Shklovskii, Critical behaviour of conductivity and dielectric constant near the metal-non-metal transition threshold, Phys. Status Solidi (b) 76 (2) (1976) 475–485, http://dx.doi.org/10.1002/pssb.2220760205. http://dx.doi.org/10.1002/pssb.2220760205.

[11] J.C.M. Garnett, Colours in metal glasses and in metallic films, Philos. Trans. R. Soc. Lond. A Math. Phys. Eng. Sci. 203 (359–371) (1904) 385–420, http://dx.doi.org/10.1098/rsta.1904.0024.

[12] D.S. McLachlan, M. Blaszkiewicz, R.E. Newnham, Electrical resistivity of composites, J. Am. Ceram. Soc. 73 (8) (1990) 2187–2203, http://dx.doi.org/10.1111/j.1151-2916.1990.tb07576.x. http://dx.doi.org/10.1111/j.1151-2916.1990.tb07576.x.

[13] C. Brosseau, Generalized effective medium theory and dielectric relaxation in particle-filled polymeric resins, J. Appl. Phys. 91 (5) (2002) 3197–3204, http://dx.doi.org/10.1063/1.1447307. http://scitation.aip.org/content/aip/journal/jap/91/5/10.1063/1.1447307.

[14] B. De Vivo, P. Lamberti, G. Spinelli, V. Tucci, A morphological and structural approach to evaluate the electromagnetic performances of composites based on random networks of carbon nanotubes, J. Appl. Phys. 115 (15) (2014), http://dx.doi.org/10.1063/1.4871670. http://scitation.aip.org/content/aip/journal/jap/115/15/10.1063/1.4871670.

[15] X. Sun, M. Song, Numerical simulations of the effect of microstructure on ac conductivity of mwcnt/polymer nanocomposites, Macromol. Theory Simul. 19 (1) (2010) 57–63.

[16] F. Nilsson, U. Gedde, M. Hedenqvist, Modelling the relative permittivity of anisotropic insulating composites, Compos. Sci. Technol. 71 (2) (2011) 216–221, http://dx.doi.org/10.1016/j.compscitech.2010.11.016. http://www.sciencedirect.com/science/article/pii/S0266353810004550.

[17] J.W. Evans, Random and cooperative sequential adsorption, Rev. Mod. Phys. 65 (1993) 1281–1329, http://dx.doi.org/10.1103/RevModPhys.65.1281. http://link.aps.org/doi/10.1103/RevModPhys.65.1281.

[18] V. Myroshnychenko, C. Brosseau, Finite-element modeling method for the prediction of the complex effective permittivity of two-phase random statistically isotropic heterostructures, J. Appl. Phys. 97 (4) (2005), http://dx.doi.org/10.1063/1.1835544. http://scitation.aip.org/content/aip/journal/jap/97/4/10.1063/1.1835544.

[19] V. Myroshnychenko, C. Brosseau, Finite-element method for calculation of the effective permittivity of random inhomogeneous media, Phys. Rev. E 71 (2005) 016701, http://dx.doi.org/10.1103/PhysRevE.71.016701. http://link.aps.org/doi/10.1103/PhysRevE.71.016701.

[20] V. Myroshnychenko, C. Brosseau, Effective complex permittivity of two-phase random composite media: A test of the two exponent phenomenological percolation equation, J. Appl. Phys. 103 (8) (2008), http://dx.doi.org/10.1063/1.2907769. http://scitation.aip.org/content/aip/journal/jap/103/8/10.1063/1.2907769.

[21] V. Myroshnychenko, C. Brosseau, Possible manifestation of nonuniversality in some continuum percolation systems, J. Phys. D Appl. Phys. 41 (9) (2008) 095401.

[22] D. Bychanok, P. Kuzhir, S. Maksimenko, S. Bellucci, C. Brosseau, Characterizing epoxy composites filled with carbonaceous nanoparticles from dc to microwave, J. Appl. Phys. 113 (12) (2013), http://dx.doi.org/10.1063/1.4798296. http://scitation.aip.org/content/aip/journal/jap/113/12/10.1063/1.4798296.

[23] C.A. Poland, R. Duffin, I. Kinloch, A. Maynard, W.A.H. Wallace, A. Seaton, V. Stone, S. Brown, W. MacNee, K. Donaldson, Carbon nanotubes introduced into the abdominal cavity of mice show asbestos-like pathogenicity in a pilot study, Nat. Nano 3 (7) (2008) 423–428. http://dx.doi.org/10.1038/nnano.2008.111.

[24] S.-E. Lee, O. Choi, H.T. Hahn, Microwave properties of graphite nanoplatelet/epoxy composites, J. Appl. Phys. 104 (3) (2008), http://dx.doi.org/10.1063/1.2965195. http://scitation.aip.org/content/aip/journal/jap/104/3/10.1063/1.2965195.

[25] M. Sarto, A. D'Aloia, A. Tamburrano, G. De Bellis, Synthesis, modeling, and experimental characterization of graphite nanoplatelet-based composites for emc applications, IEEE Trans. Electromagn. Compat. 54 (1) (2012) 17–27, http://dx.doi.org/10.1109/TEMC.2011.2178853.

[26] S. Stankovich, D.A. Dikin, R.D. Piner, K.A. Kohlhaas, A. Kleinhammes, Y. Jia, Y. Wu, S.T. Nguyen, R.S. Ruoff, Synthesis of graphene-based nanosheets via chemical reduction of exfoliated graphite oxide, Carbon 45 (7) (2007) 1558–1565, http://dx.doi.org/10.1016/j.carbon.2007.02.034. http://www.sciencedirect.com/science/article/pii/S0008622307000917.

[27] J. Li, J.-K. Kim, M.L. Sham, Conductive graphite nanoplatelet/epoxy nanocomposites: effects of exfoliation and uv/ozone treatment of graphite, Scr. Mater. 53 (2) (2005) 235–240.

[28] L. Guadagno, M. Raimondo, L. Vertuccio, M. Mauro, G. Guerra, K. Lafdi, B. De Vivo, P. Lamberti, G. Spinelli, V. Tucci, Optimization of graphene-based materials outperforming host epoxy matrices, RSC Adv. 5 (46) (2015) 36969–36978.

[29] A. Yu, P. Ramesh, M.E. Itkis, E. Bekyarova, R.C. Haddon, Graphite nanoplatelet-epoxy composite thermal interface materials, J. Phys. Chem. C 111 (21) (2007) 7565–7569.

[30] M.-T. Hung, O. Choi, Y.S. Ju, H.T. Hahn, Heat conduction in graphite-nanoplatelet-reinforced polymer nanocomposites, Appl. Phys. Lett. 89 (2) (2006), http://dx.doi.org/10.1063/1.2221874. http://scitation.aip.org/content/aip/journal/apl/89/2/10.1063/1.2221874.

[31] J.-K. Kim, C. Hu, R.S. Woo, M.-L. Sham, Moisture barrier characteristics of organoclayepoxy nanocomposites, Compos. Sci. Technol. 65 (5) (2005) 805–813, http://dx.doi.org/10.1016/j.compscitech.2004.10.014 papers presented at the European Materials Research Society 2004 Spring Meeting: Nano-Composites for Space and Infrastructure Applications, http://www.sciencedirect.com/science/article/pii/S0266353804002878.

[32] D. van der Putten, J.T. Moonen, H.B. Brom, J.C.M. Brokken-Zijp, M.A.J. Michels, Evidence for superlocalization on a fractal network in conductive carbon-blackpolymer composites, Phys. Rev. Lett. 69 (1992) 494–497, http://dx.doi.org/10.1103/PhysRevLett.69.494. http://link.aps.org/doi/10.1103/PhysRevLett.69.494.

[33] C. Brosseau, P. Molini, F. Boulic, F. Carmona, Mesostructure, electron paramagnetic resonance, and magnetic properties of polymer carbon black composites, J. Appl. Phys. 89 (12) (2001) 8297–8310, http://dx.doi.org/10.1063/1.1371938. http://scitation.aip.org/content/aip/journal/jap/89/12/10.1063/1.1371938.

[34] A. Pyushch, J. Macutkevic, J. Banys, D. Bychanok, S. Maksimenko, A. Cataldo, F. Micciulla, S. Bellucci, Electromagnetic properties of graphene nano

platelets/epoxy composites in whide temperature range, in: Proceedings of International Conference Nanomeeting-2015, 26-29 May 2015, World Scientific, 2015, pp. 233–235.
[35] K.-M. Jäger, D. McQueen, J. Vilcakova, Ac conductance and capacitance of carbon black polymer composites during thermal cycling and isothermal annealing, J. Phys. D Appl. Phys. 35 (10) (2002) 1068.
[36] P. Mather, K. Thomas, Carbon black/high density polyethylene conducting composite materials: part I structural modification of a carbon black by gasification in carbon dioxide and the effect on the electrical and mechanical properties of the composite, J. Mater. Sci. 32 (2) (1997) 401–407.
[37] S. Barrau, P. Demont, A. Peigney, C. Laurent, C. Lacabanne, Dc and ac conductivity of carbon nanotubes-polyepoxy composites, Macromolecules 36 (14) (2003) 5187–5194.
[38] J. Macutkevic, P. Kuzhir, A. Paddubskaya, S. Maksimenko, J. Banys, A. Celzard, V. Fierro, S. Bistarelli, A. Cataldo, F. Micciulla, S. Bellucci, Electrical transport in carbon black-epoxy resin composites at different temperatures, J. Appl. Phys. 114 (3) (2013) 033707, http://dx.doi.org/10.1063/1.4815870. http://scitation.aip.org/content/aip/journal/jap/114/3/10.1063/1.4815870.
[39] J. Macutkevic, P.P. Kuzhir, A.G. Paddubskaya, J. Banys, S.A. Maksimenko, E. Stefanutti, F. Micciulla, S. Bellucci, Broadband dielectric/electric properties of epoxy thin films filled with multiwalled carbon nanotubes, J. Nanophot. 7 (1) (2013), http://dx.doi.org/10.1117/1.JNP.7.073593, 073593–073593, http://dx.doi.org/10.1117/1.JNP.7.073593.
[40] X. He, J. Du, Z. Ying, H. Cheng, Positive temperature coefficient effect in multiwalled carbon nanotube/high-density polyethylene composites, Appl. Phys. Lett. 86 (6) (2005) 062112.
[41] J.-F. Gao, D.-X. Yan, B. Yuan, H.-D. Huang, Z.-M. Li, Large-scale fabrication and electrical properties of an anisotropic conductive polymer composite utilizing preferable location of carbon nanotubes in a polymer blend, Compos. Sci. Technol. 70 (13) (2010) 1973–1979.
[42] A. Dabrowska, S. Bellucci, A. Cataldo, F. Micciulla, A. Huczko, Nanocomposites of epoxy resin with graphene nanoplates and exfoliated graphite: synthesis and electrical properties, Phys. Status Solidi (b) 251 (12) (2014) 2599–2602, http://dx.doi.org/10.1002/pssb.201451175. http://dx.doi.org/10.1002/pssb.201451175.
[43] S. Bellucci, M. Bozzi, A. Cataldo, R. Moro, D. Mencarelli, L. Pierantoni, Graphene as a tunable resistor, in: Semiconductor Conference (CAS), 2014 International, 2014, pp. 17–20, http://dx.doi.org/10.1109/SMICND.2014.6966380.
[44] L. Pierantoni, M. Bozzi, R. Moro, D. Mencarelli, S. Bellucci, On the use of electrostatically doped graphene: analysis of microwave attenuators, in: 2014 International Conference on Numerical Electromagnetic Modeling and Optimization for RF, Microwave, and Terahertz Applications (NEMO), 2014, pp. 1–4, http://dx.doi.org/10.1109/NEMO.2014.6995716.
[45] L. Pierantoni, D. Mencarelli, M. Bozzi, R. Moro, S. Bellucci, Graphene-based electronically tunable microstrip attenuator, in: Microwave Symposium (IMS), 2014 IEEE MTT-S International, 2014, pp. 1–3, http://dx.doi.org/10.1109/MWSYM.2014.6848645.
[46] L. Pierantoni, D. Mencarelli, M. Bozzi, R. Moro, S. Moscato, L. Perregrini, F. Micciulla, A. Cataldo, S. Bellucci, Theoretical and experimental characterization of a broadband microwave attenuator based on few layer graphene flakes, in press, IEEE Trans. Microw. Theory Tech. 63 (8) (2015) 2491–2497, http://dx.doi.org/10.1109/TMTT.2015.2441062.
[47] J. Baker-Jarvis, E. Vanzura, W. Kissick, Improved technique for determining complex permittivity with the transmission/reflection method, IEEE Trans. Microw. Theory Tech. 38 (1990) 1096–1103, http://dx.doi.org/10.1109/22.57336.
[48] B.-K. Chung, Dielectric constant measurement for thin material at microwave frequencies, progress, Electromagn. Res. 75 (2007) 239–252.
[49] E. Nielsen, Scattering by a cylindrical post of complex permittivity in a waveguide, IEEE Trans. Microw. Theory Tech. 17 (3) (1969) 148–153, http://dx.doi.org/10.1109/TMTT.1969.1126913.
[50] A.K. Jonscher, Universal Relaxation Law: a Sequel to Dielectric Relaxation in Solids, Chelsea Dielectrics Press, 1996.
[51] A.K. Jonscher, The universal'dielectric response, Nature 267 (1977) 673–679.
[52] A. Jonscher, M. Frost, Weakly frequency-dependent electrical conductivity in a chalcogenide glass, Thin Solid Films 37 (2) (1976) 267–273. http://www.sciencedirect.com/science/article/pii/0040609076901930.
[53] K. Ahmad, W. Pan, S.-L. Shi, Electrical conductivity and dielectric properties of multiwalled carbon nanotube and alumina composites, Appl. Phys. Lett. 89 (13) (2006), http://dx.doi.org/10.1063/1.2357920. http://scitation.aip.org/content/aip/journal/apl/89/13/10.1063/1.2357920.
[54] C.-W. Nan, Physics of inhomogeneous inorganic materials, Prog. Mater. Sci. 37 (1) (1993) 1–116, http://dx.doi.org/10.1016/0079-6425(93)90004-5. http://www.sciencedirect.com/science/article/pii/0079642593900045.
[55] M. Panda, V. Srinivas, A. Thakur, On the question of percolation threshold in polyvinylidene fluoride/nanocrystalline nickel composites, Appl. Phys. Lett. 92 (13) (2008) 132905.
[56] Z.-M. Dang, Y.-H. Lin, C.-W. Nan, Novel ferroelectric polymer composites with high dielectric constants, Adv. Mater. 15 (19) (2003) 1625–1629.
[57] J. Macutkevic, J. Banys, A. Matulis, Determination of the distribution of the relaxation times from dielectric spectra, Nonlinear Anal. Model. Control 9 (1) (2004) 75–88.
[58] S. Torquato, Nearest-neighbor statistics for packings of hard spheres and disks, Phys. Rev. E 51 (4) (1995) 3170.
[59] P. Sheng, E.K. Sichel, J.I. Gittleman, Fluctuation-induced tunneling conduction in carbon-polyvinylchloride composites, Phys. Rev. Lett. 40 (1978) 1197–1200, http://dx.doi.org/10.1103/PhysRevLett.40.1197. http://link.aps.org/doi/10.1103/PhysRevLett.40.1197.